Journal of Electroanalytical Chemistry 651 (2011) 204–210

Contents lists available at ScienceDirect

Journal of Electroanalytical Chemistry

journal homepage: www.elsevier.com/locate/jelechem

Microfluidic-enzymatic biosensor with immobilized tyrosinase for electrochemical detection of pipemidic acid in pharmaceutical samples

Franco A. Bertolino [a], Irma E. De Vito [a], Germán A. Messina [a], Héctor Fernández [b], Julio Raba [a,*]

[a] INQUISAL, Departamento de Química. Universidad Nacional de San Luis, CONICET. Chacabuco 917. D5700BWS. San Luis, Argentina
[b] Departamento de Química. Facultad de Ciencias Exactas, Físico-Químicas y Naturales. Universidad Nacional de Río Cuarto. Agencia Postal No. 3, 5800 Río Cuarto, Argentina

ARTICLE INFO

Article history:
Received 16 June 2010
Received in revised form 13 November 2010
Accepted 2 December 2010
Available online 10 December 2010

Keywords:
Microfluidic
Enzymatic sensor
Pipemidic acid
Gold electrode
Pharmaceutical samples

ABSTRACT

The present article describes the development of a microfluidic-enzymatic sensor with electrochemical detection for the quantification of pipemidic acid (PA), which is a synthetic quinolone used as antibacterial agent. This property of the quinolones is associated with their potential to inhibit topoisomerase II (DNA gyrase) of bacteria. PA detection in pharmaceutical samples was based in the use of tyrosinase enzyme [EC 1.14.18.1] that was immobilized on 3-aminopropyl-modified-controlled-pore glass (APCPG) packet in a central channel (CC) of the microfluidic-enzymatic device. This enzyme catalyzes the oxidation of catechol to o-benzoquinone, whose back electrochemical reduction was detected at gold electrode surface at 0 V vs. Ag/AgCl. Thus, when PA was added to the solution, this piperazine-containing compound participates in a Michael addition reaction with o-benzoquinone to form the corresponding amino-quinone derivative, as result of this interaction the peak current obtained for o-benzoquinone reduction decreased proportionally to the increase of the PA concentration. The recovery of PA from four samples ranged from 97.50% to 102.50%. This method could be used to determine the PA concentration in the range 0.02–70 μM (r = 0.998) with a limit of detection of 18 nM. This method was successfully applied for the analysis of PA in pharmaceutical formulations.

© 2010 Elsevier B.V. All rights reserved.

1. Introduction

Pipemidic acid (PA) (Scheme 1), 8-ethyl-5,8-dihydro-5-oxo-2-(1-piperazinyl) pyrido[2,3-*d*]pyrimidine-6-carboxylic acid, is a synthetic quinolone that belongs to the first generation of this kind of compounds, which is used as antibacterial agent. The antibacterial property of the quinolones is associated with their potential to inhibit the bacterial topoisomerase II (DNA gyrase). Their effectiveness depends on the quinolone structure [1]. PA is widely used for the treatment of urinary tract infections, showing high activity against gram-positive and gram-negative bacteria.

Several methods for the determination of PA have been developed, as luminescence techniques [2–6] including lanthanide-sensitized luminescence [7,8], Optosensor [9] and HPLC [10,11].

The use of microfluidic-enzymatic sensors with electrochemical detection represents an interesting option to be considered for PA determination, because these devices offer many potential advantages, including a reduced reagents consumption, smaller analysis volumes, faster analysis times, and increased instrument portability [12]. Also, in recent years, there has been growing interest in the development of microfluidic lab-on-a-chip systems for analytical chemistry, biology, biomedical and clinical diagnostics applications. These systems have been subject of several recent reviews [13–20]. Microfluidic devices allow the incorporation of particles as solid support, for immobilizing enzymes, antibodies or antigens, which are packed in a microchannel increasing of this manner the surface area [21,22]. For these reasons, we have developed a very sensitive device based in the presence of the tyrosinase immobilized on APCPG particles contained into the CC of the microfluidic-enzymatic-systems, where occurs the enzymatic reaction for indirect-PA determination.

Tyrosinase, a two copper-containing enzyme, catalyzes the o-hydroxylation of monophenols (monophenolase activity) and the oxidation of o-diphenols to o-quinones (diphenolase activity) [23–25]. Over the past decades several reports on the tyrosinase action mechanism have been published [26–29], although major advances in understanding of this mechanism have only been obtained by studying the nature of the copper site [29–31]. This enzyme has been used extensively in the development of biosensors for the detection of phenolic compounds [32–38].

The inhibition of the tyrosinase activity was utilized in the determination of toxic pollutants in environmental and biological samples [39,40]. Tyrosinase has also been used in combination with a PQQ-dependent dehydrogenase for the determination of alkaline phosphatase [41,42] and in combination with a hydroxylase for NADH and NADPH measurements [43,44].

* Corresponding author. Tel.: +54 2652 425385; fax: +54 2652 430224.
E-mail address: jraba@unsl.edu.ar (J. Raba).

1572-6657/$ - see front matter © 2010 Elsevier B.V. All rights reserved.
doi:10.1016/j.jelechem.2010.12.007

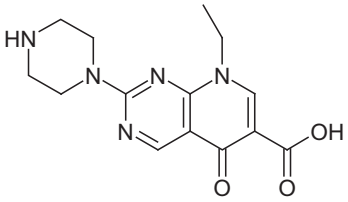

Scheme 1. Chemical structure of the pipemidic acid.

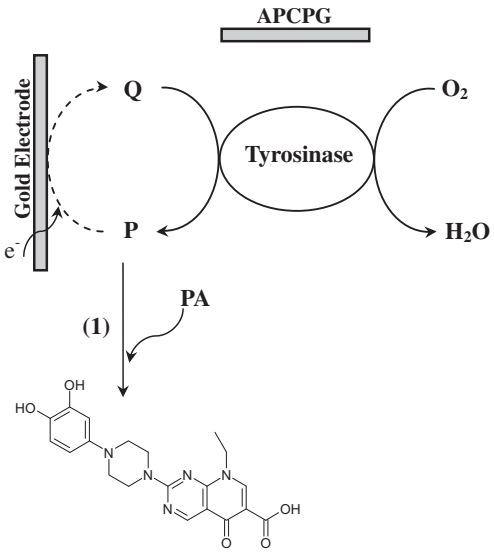

Scheme 2. Schematic representations of the reduction wave of the enzymatic process between catechol (Q), o-benzoquinone (P), pipemidic acid (PA) and tyrosinase.

The measuring principle (Scheme 2) of this microfluidic-enzymatic-sensor, for the determination of PA, is based on the presence of tyrosinase immobilized on APCPG particles contained in the central channel (CC), which catalyze the oxidation of catechol (Q) to o-benzoquinone (P), which was reduced back to catechol on the surface of the gold electrode (at 0 V vs. Ag/AgCl) present at the end of the CC. The detection of PA is accomplished by suppressing the substrate recycling process between tyrosinase and the electrode (Scheme 2, denoted by the dotted arrow). Therefore, the detection principle is similar to sensors based on substrate competition and it allows a rapid determination of PA, minimizing the waste of expensive reagents. Also, it does not require highly skilled technicians or expensive equipment [45]. The results were compared with those obtained by high-performance liquid chromatography (HPLC).

2. Experimental

2.1. Reagents and solutions

All reagents used were of analytical grade. The enzyme tyrosinase (from mushroom, EC 1.14.18.1, 2000 U mg^{-1}) was purchased from Sigma Chemical Co. (St. Louis, MO, USA). The enzyme concentration was determined taking the value of M_r as 120,000. Glutaraldehyde (25% aqueous solution) was purchased from Merck, Darmstadt, Germany. Aminopropyl-modified controlled-pore glass (APCPG), 1400 Å in mean pore diameter and 24 m^2 mg^{-1} in surface area was from Electro Nucleonics (Fairfield, NJ, USA) and contained 48.2 μmol g^{-1} amino groups. Catechol, 4-methylcatechol and 4-tert-butylcatechol were purchased from Sigma Chemical Co. (St. Louis, MO, USA) and generally used within 1 h. Pipemidic acid (PA) (Merck Lab.) stock standard solution was prepared with exact measurement of pipemidic acid dissolved in 0.02 N NaOH. This solution was stable for at least 1 week if stored away from light, at 4 °C. Working solutions were prepared by appropriate dilutions with a 0.1 M phosphate buffer (pH 7.00). All other reagents employed were of analytical grade and were used without further purification. All solutions were prepared with ultra-high-quality water obtained from a Barnstead Easy pure RF compact ultra pure water system, and samples were diluted to the desired concentrations using a 10 mL Metrohm E 485 burette.

2.2. Flow-through sensor/detector unit

The main body of the sensor was made of Plexiglas. Fig. 1 illustrates the design of the microfluidic device and the detection system. The gold electrode is at the end of the central channel (CC); the cleaning and preconditioning of this electrode was made using cyclic voltammetry in 0.5 M sulphuric acid by 3-fold cycling in the potential range between −300 and 1300 mV at 100 mV s^{-1} scan rate. Typically, the CC carried 0.3 mg of controlled-pore glass, and the end of the CC was blocked with glass fibers. The diameter of the CC was 150 μm and the diameter of the accessory channels was 100 μm. All solutions and reagent temperatures were conditioned before the experiment using a Vicking Masson II laboratory water bath (Vicking SRL, Buenos Aires, Argentina). Amperometric detection was performed using a BAS LC-4C potentiostat and a BAS 100 B/W (electrochemical analyzer Bioanalytical System, West Lafayette, IN, USA) was used for voltammetric determinations. The potential applied to the gold electrode for the functional group detection was 0 V vs. the Ag/AgCl wire pseudo-reference electrode and a Pt wire was the counter electrode. At this potential, a catalytic current was well established. Pumps (Baby Bee Syringe Pump, Bioanalytical Systems) were used for pumping, sample introduction, and stopping flow. The pump tubing was Tygon (Fisher Accu-Rated, 1.0 mm i.d., Fisher Scientific Co., Pittsburgh, PA).

All pH measurements were made with an Orion Expandable Ion Analyzer (Orion Research Inc., Cambridge, MA, USA) Model EA 940 equipped with a glass combination electrode (Orion Research Inc.). Absorbance was determined with a Bio-Rad Benchmark microplate reader (Japan) and Beckman DU 520 General UV/VIS spectrophotometer.

The HPLC experiments were performed with a Beckman model 332 liquid chromatography equipped with a variable wavelength detector model 164 operated at $\lambda = 278$ nm. The retention times as well as peak area measurements were obtained with a Varian 4290 integrator. Experiments were done at room temperature and a Phenosphere 5 μm ODS-2 C18 column (250 × 4.6 mm) [10,11,46–48] was used in all experiments with a flow rate of 1.5 mL min^{-1}. The mobile phase consisted of acetonitrile-methanol-acetate buffer (pH 3.6; 0.05 M) (10 + 30 + 60, v/v/v) containing 1% v/v acetic acid. Quantitative data were calculated from the linear regression of external standards of PA, relating peak area and concentration.

2.3. Tyrosinase immobilization

The microfluidic-enzymatic biosensor was prepared by immobilizing tyrosinase on 3-aminopropyl-modified controlled-pore glass (APCPG). The APCPG was allowed to react with an aqueous solution of 5% (w/w) glutaraldehyde at pH 10.00 (0.2 M carbonate) for 2 h at room temperature. After washed with purified water and 0.1 M phosphate buffer of pH 7.00, the enzyme (5.0 mg of enzyme preparation in 0.25 mL of 0.1 M phosphate buffer, pH 7.00) was coupled with residual aldehyde groups in phosphate buffer

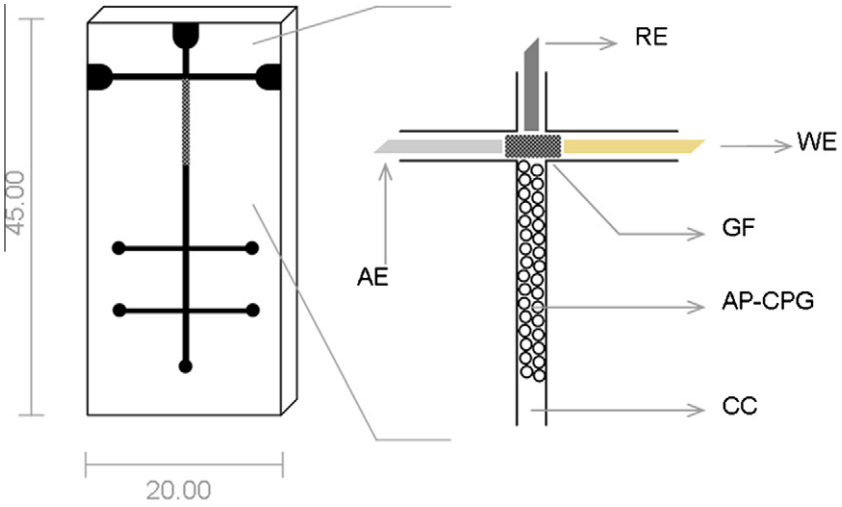

Fig. 1. Schematic representation of the microfluidic biosensor. RE, reference electrode; AE, counter electrode; WE, gold working electrode; GF, glass fiber; APCPG, 3-aminopropyl-modified controlled-pore glass; CC, central channel.

(0.1 M, pH 7.00) overnight at 4 °C. The immobilized enzyme preparation was then washed with phosphate buffer (pH 7.00) and stored in the same buffer at 4 °C between uses. The biosensor was prepared by packing 0.3 mg of modified APCPG in the CC. The immobilized tyrosinase preparations were perfectly stable throughout at least 1 month of daily use.

2.4. Preparation and analysis of pharmaceutical samples

The contents of 10 capsules or envelopes were weighed from each dosage forms and powdered. Equivalent amount to 100 mg of PA was weighed and transferred to a 250 mL volumetric flask, and 20 mL of 0.02 N NaOH solution was added. The flask was sonicated for 10 min and filled with 0.1 M phosphate buffer, pH 7.00. A small amount of non-dissolving excipients settled at the bottom of the flask. Appropriated solutions were prepared by taking suitable aliquots of the clear supernatant and diluting them with 0.1 M phosphate buffer, pH 7.0; these solutions where later injected by syringe pumps system into of CC of the microfluidic device and the amperometric measurements were performed at 0 V and the resulting cathodic current was displayed on the *x–y* recorder.

2.5. Preparation of synthetic samples

Synthetic samples were prepared into a 100 mL calibrated flasks by spiking a placebo (mixture of the capsule excipients) with an accurately amount of PA at a concentration similar to formulation concentration. Then, the procedure described for the preparation of pharmaceuticals was followed.

2.6. Dosage forms of PA

(1) Priper 0.400 g hard gelatin capsules (Ivax) and (2) Priper powder 1 g envelopes (Ivax).

2.7. Sample preparation for HPLC assay

Aliquots (400 μL) of drug-free solution were spiked with aqueous standard PA solutions (1000 μL). The samples were centrifuged at 3500 rpm for 15 min and subsequent transfer of supernatants to clean Eppendorf vials. The supernatants were evaporated to dryness under a stream of nitrogen in a water bath at 45 °C and the residues were reconstituted with a 100 μL volume of an aqueous 0.1 μg mL^{-1} solution of anthranilic acid. Repetitive analyses ($n = 6$) of the resulting solutions at each concentration level were performed.

3. Results and discussion

3.1. Enzymatic process

Reactions catalyzed by enzymes have long been used for analytical purposes in the determination of different analytes, such as substrates, inhibitors and also the enzymes. In this paper, we apply a tyrosinase biosensor for a highly sensitive determination of PA in pharmaceutical formulations. The measuring principle of this biosensor for the determination of PA is shown in Scheme 2. First, the tyrosinase immobilized on APCPG particles catalyzes the oxidation of Q to P [49,50], whose electrochemical reduction back to Q was obtained at a potential of 0 V. Second, the detection of PA is accomplished by suppressing the substrate recycling process between tyrosinase and the electrode (denoted by the dotted arrow), which leads to a decreasing of the current obtained proportionally to the increase of PA concentration. Therefore, the detection principle is similar to biosensors based on substrate competition [45,51,52].

When piperazine-containing compound is added to the solution, it readily undergo a reaction with the quinone derivative P, through the Michael type addition, decreasing the current obtained proportionally to the increase of piperazine-containing compound concentration [53].

The initial reaction in the sequence (Q ⇌ P) is well established [54–56] with NMR, pulse radiolysis and a number of electrochemical techniques used to probe the mechanism. The potential analytical utility offered by the second step (1) of Scheme 2 as a method for detecting PA is explored in this paper.

3.2. Electrochemical study of catechol in the absence and presence of pipemidic acid

Cyclic voltammetry of a 1 mM solution of Q in an aqueous solution containing 0.1 M phosphate buffer pH 7.00 as a supporting electrolyte, shows one anodic (A_1) and a corresponding cathodic peak (C_1), which correspond to the transformation of Q to P and vice versa within a quasi-reversible two-electron process (Fig. 2, curve *a*). A peak current ratio (Ip^{C_1}/Ip^{A_1}) of near unity, particularly

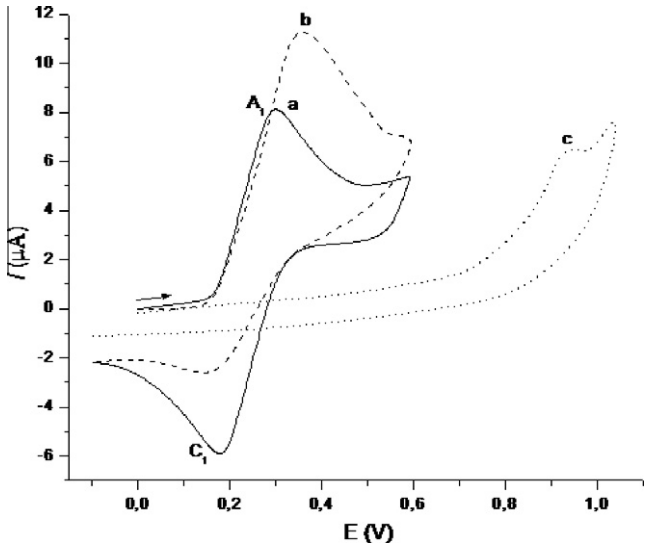

Fig. 2. Cyclic voltammograms of 1.0 mM Q: (a) in the absence; (b) in the presence of 0.75 mM PA; and (c) 0.75 mM PA in the absence of Q, at gold electrode (1.6 mm diameter) in aqueous solution containing 0.1 M phosphate buffer (pH 7.00). Scan rate: 100 mV s^{-1}; *T*: 25 ± 1 °C.

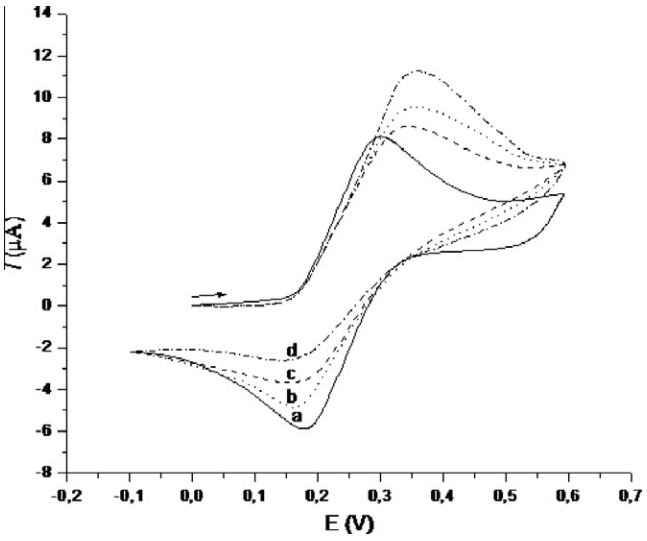

Fig. 3. Typical voltammograms of 1.0 mM Q at a gold electrode (1.6 mm diameter) in aqueous solution containing 0.1 M phosphate buffer (pH 7.00) at various PA concentrations, C_{PA}: a) 0.0; b) 0.25; c) 0.50; d) 0.75 mM; Scan rate: 100 mV s^{-1}, *T*: 25 ± 1 °C.

during the repetitive recycling of potential, can be considered as a criterion for the stability of o-quinone produced at the surface of the electrode under the experimental conditions. In other words, all possible hydroxylations [57–60] or dimerization [61,62] reactions are too slow to be observed on the time-scale of cyclic voltammetry. The oxidation of Q in the presence of PA as a nucleophile was also studied. Fig. 2, curve *b*, shows the cyclic voltammogram obtained for a 1 mM solution of Q in presence of 0.75 mM PA. The voltammogram exhibits an anodic peak at 359 mV vs. Ag/AgCl/3 M NaCl, while the cathodic counterpart of the anodic peak A_1 tends to disappear under this condition. A voltammogram of PA in the absence of Q is depicted in Fig. 2, curve *c*. An oxidation wave appears at potentials much more positive (about 0.8–1.0 V) with respect to the one of Q in the presence of PA. The influence of increasing PA concentration on the electrochemical behavior of Q was also investigated and subsequent responses are shown in the Fig. 3. The height of the oxidation peak was found to increase with increasing additions of PA, resulting in the loss of the corresponding reduction peak in agreement with the ECE type mechanism proposed in Scheme 2. Hence, the increase in the oxidation peak height is attributed to the oxidation of Q–PA adducts that arises through the electrochemically initiated reaction (Scheme 2). In fact, once Q is formed, could react with a variety of nucleophilic reagents, as those possessing amino (–N–) and sulfhydryl (–SH) groups [63]. For this reason, in the case of the Q oxidation in presence of PA, only the N-adduct (Q–PA) is formed [53,64]. Given that the direct oxidation of PA at the electrode does not occur within the potential window studied (Fig. 2, curve *c*), the increase in the magnitude of the Q oxidation peak can be attributed solely to the Q–PA adduct formation.

The influence of pH on the peak potential (*Ep*) of the reaction was assessed through examining the electrode response to PA–Q obtained in solutions buffered between pH 4 and pH 8. The position of the redox couple was found to be dependent upon pH with a shift of 61 mV pH^{-1}, indicative of *n* electron *n* proton behavior with *n* likely to be two [65]. A quantitative evaluation of the Q change peak current (ΔIp) response to increasing additions of PA as a function of solution pH (data not showed) was accomplished. The measured ΔIp is the difference between the reduction current (from addition of Q) and the current due to the addition of PA (from addition of Q + PA). The response decreased steadily as the acidity of the solution was increased. This can be attributed to the fact that as the pH of the solution was lowered, the piperazine functionality increasing protonated (PA, $pK_a \sim 8.20$) and hence the nucleophilic character of the piperazine moiety diminished. Increasing the pH clearly improves the response but an operational limit is reached once neutral conditions prevail. Alkaline solution severely compromises the enzyme stability as well as the response of increased presence of nucleophilic hydroxyl ions compete with the less prevalent piperazine compound. Therefore, the pH value used was 7.00 in 0.1 M phosphate buffer in concordance with the steadier pH of the enzyme.

3.3. Redox indicator selection

The enzymatic generated reaction clearly represents a sensitive and selective method for the determination of secondary amines but the true strength of the protocol lies in the generic nature of the indicating process. This was highlighted through the examination of a further three derivatives of varying chemical functionality. The compounds investigated are shown in the Table 1 along with a summary of their electrochemical properties. While the chemical composition has been varied, each derivative retained the capacity for electrochemical conversion to a quinoid intermediate and hence was generally amenable to reaction with piperazine derivatives. Changing the chemical composition of the parent indicator species can alter the electrochemical properties of the system and hence the nature of the resulting analytical signal. As can be seen from this table, the chemical reaction between PA and quinone derivative from 4-tert-butylcatechol is sufficiently slow to

Table 1
Electrochemical detection of PA via tyrosinase-microfluidic biosensor with redox substrate: analytical parameters.

Compounds investigated	E_f° [a] (V)	Pipemidic acid	
		Range (μM)	DL[b] (μM)
Catechol	0.238	0.02–70	0.018
4-Methylcatechol	0.182	0.09–60	0.062
4-Tert-buthylcatechol	0.134	No reaction	No reaction

[a] E_f°: formal potential.
[b] DL: detection limit; *n* = 6.

be observed on the time-scale of cyclic voltammetry. This fact could be envisaged due the increased steric bulk of the tert-butyl moiety prevents the PA addition within the time-scale of the experiment. By the other way, there is a decrease in the range of concentrations and an increase in the detection limit of the 4-methylcatechol system when compared to the response obtained with catechol; therefore, the last one is the selected compound for this work.

3.4. Optimum conditions

For the development of the microfluidic sensor, we must take into account the optimization of different variables, which we detail below.

3.4.1. Effect of flow rate

The optimal flow rate was determined by analyzing a standard of 25 μM of PA at different flow rates and evaluating the current generated during the enzymatic reaction. As shown in Fig. 4, flow rates from 1 to 6 μL min^{-1} had little effect on enzymatic reaction. Conversely, when the flow rate exceeded the 7 μL min^{-1}, the signal was suddenly reduced. Therefore, a flow rate of 5 μL min^{-1} was used for injections of reagents and washing buffer. The rate of enzymatic response under flow conditions was studied in the pH range 4–8 and showed a maximum value of activity at pH 7.0.

3.4.2. Effect of sample size

The sample volume was studied in the range 1–30 μL. The rate of response increased linearly and sensitivity was almost triplicated when the sample volume was 1–15 μL, insignificant differences can be observed when sample size is bigger to 15 μL. For convenience a sample volume of 15 μL was used to evaluate other parameters.

3.5. PA measurement with microfluidic-enzymatic sensor

The working potential was selected using the same cyclic voltammogram showed before (Fig. 2, curve *a*) for the couple Q/P at a gold electrode in phosphate buffer. For potentials values below 0 V, the cathodic current became independent of the applied potential; therefore, this value was chosen as working potential. Furthermore, at this potential, a less contribution of the electroactive interferences present in pharmaceutical sample is expected.

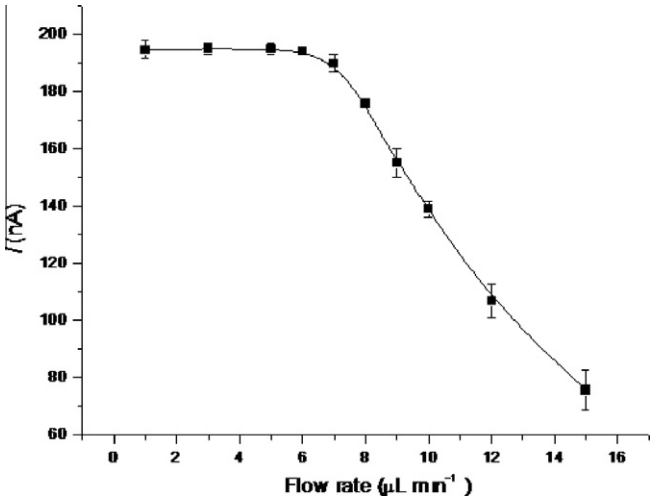

Fig. 4. Effect of the flow rates from 1 to 15 μL min^{-1} on analysis of a 25 μM PA standard.

The performance of the tyrosinase-microfluidic biosensor for the measurement of PA concentrations was characterized. Firstly, a solution containing 1 mM Q in 0.1 M phosphate buffer (pH 7.00) was injected into the CC of the biosensor at flow rate of 5 μL min^{-1} for 3 min, thus, a large reduction current was observed due to the presence of the quinone derivative. After that, the device was washed with 0.1 M phosphate buffer (pH 7.00) at flow rate of 5 μL min^{-1} for 3 min. Then a solution containing 1 mM Q and several PA concentrations were injected at flow rate of 5 μL min^{-1} for 3 min generating a reduction current. In this step, tyrosinase immobilized on APCPG in the CC converts catechol (Q) to o-benzoquinone (P), which was reduced to Q on the surface of the gold electrode at the end of the CC. The detection of the PA is accomplished by suppressing the substrate recycling process between tyrosinase and the electrode surface. For the next analysis, the sensor was rinsed with 0.1 M phosphate buffer (pH 7.00) at a flow rate of 5 μL min^{-1} for 3 min. After six determinations, the gold electrode was cleaned and preconditioned as indicated in Section 2. A PA calibration plot was obtained by plotting ΔI vs. PA concentration. The background solution was buffer phosphate pH 7.0. A linear relation, ΔI (nA) = 311.37–4.443 [C_{PA}], was observed between the ΔI and the PA concentration in the range of 0.02 and 70 μM. The linear regression coefficient for this type of plot was $r = 0.998$. Detection limit (DL) was calculated as the amount of PA required to yield a net peak that was equal to three times the standard deviation (SD) of the pure Q signal. In this study, the minimal difference of concentration of PA was 18 nM. Reproducibility assays were made using repetitive standards solutions ($n = 5$) containing 1.0 mM Q and 10 μM PA, and the coefficient of variation (CV) for this study was below 3%.

The long-term stability of the enzymatic system to pharmaceutical formulations was study. In this experiment, after every five samples measured, a standard of 10 μM PA was injected to test the electrode response. There is practically no decay in the catalytic current after six samples (data not showed).

3.6. Determination of PA in pharmaceuticals formulations

Specificity is the ability of the method to measure the analyte response in the presence of all the potential interference. For the specificity test, standard solutions of tablet excipients were recorder at selected conditions. The response of the analyte with excipients was compared with the response of pure PA. It was found that the signal was not changed. Therefore, the excipients did not interfere with the quantification of PA as such in synthetic as well as commercial samples. Results are shown in Table 2.

Recovery studies were performed by adding a synthetic mixture prepared according to the manufacturer's batch formula to known amount of PA. The recovery was between 97.50% and 102.50%. These results are shown in Table 3.

The precision for PA was <4.9% within the range 0.4–1.0 g (Table 3). Precision studies were performed by adding a synthetic mixture prepared according to the manufacturer's batch formula to known amount of PA. The accuracy for PA was <2.6% (Table 3).

Table 2
Specificity results of the proposed method.

Sample No.	Pure sample (10 μM)	Synthetic capsule sample ($n = 5$) (X μM)
1	10.02	10.26
2	9.97	10.18
3	10.05	9.92
4	9.98	9.90
5	9.95	10.13
$X \pm$ S.D.[a]	9.99 ± 0.04	10.08 ± 0.16

[a] X (μM): mean ± S.D.: standard deviation.

Table 3
Accuracy and precision data for PA obtained by amperometric measurements.

Added (g)	Found (g)	Recovery (%)	Precision (g)	Accuracy[a] (% relative error)
0.40	0.39	97.50	X^b = 0.39 ± 0.01 CV[c] = 2.56	−2.5
0.60	0.61	101.70	X = 0.61 ± 0.02 CV = 3.28	1.7
0.80	0.82	102.50	X = 0.82 ± 0.04 CV = 4.88	2.5
1.00	1.02	102.00	X = 1.02 ± 0.03 CV = 2.94	2

[a] Accuracy = [(found−added)/added] × 100.
[b] X (g): mean ± S.D.: standard deviation.
[c] CV: coefficient of variation.

Table 4
Within-assay precision (five measurements in the same run for each control sample) and between-assay precision (five measurements for each control sample, repeated through three consecutive days).

Added PA (g L^{-1})	Within-assay		Between-assay	
	X[a]	CV[b]	X	CV
0.4	0.39	3.40	0.42	4.80
0.6	0.61	2.18	0.64	3.22
0.8	0.82	1.40	0.78	3.55

[a] X (g L^{-1}): mean.
[b] CV: coefficient of variation.

Table 5
Determination of amount of PA contained in commercial sample by the developed method, based on triplicate of six determinations.

Sample No.	Priper 0.4 g capsules	Priper 1.0 g powder
1	0.41	1.03
2	0.39	0.98
3	0.38	1.02
4	0.41	0.99
5	0.37	1.04
6	0.42	0.97
X[a] ± S.D.	0.39 ± 0.01	1.01 ± 0.03

[a] X (g): mean ± S.D.: standard deviation.

The precision of the electrochemical assay was checked with control samples 0.4, 0.6 and 0.8 g L^{-1} PA concentrations. The within-assay precision was tested with five measurements in the same run for each sample. These series of analyses were repeated for three consecutive days in order to estimate the between-assay precision. The results obtained are presented in Table 4. The PA assay showed good precision; the CV within-assay values were below 3.5% and the between-assay values were below 4.9%. There are no significant differences in the results, indicating that the analysis of PA tablets by the proposed method is reproducible.

The developed microfluidic-biosensor method for the PA determination was applied to two commercial preparations (Table 5). There is no need for any extraction procedure before of the analysis. No change of the current level in the presence of the excipients was observed.

The high sensitivity achieved by the proposed method, which is compared with HPLC, allows the determination of PA in pharmaceutical samples of commercial use. Results obtained for three samples are gathered in Table 6 along with results obtained by HPLC. These results were compared, and there was no significant difference between the methods.

Table 6
Results for three samples (n = 5) analyzed by two techniques.

Sample No.	Microfluidic-biosensor			HPLC		
	1	2	3	1	2	3
C_{PA} (μM)[a]	0.50	5.00	50.00	0.50	5.00	50.00
X (μM)[b]	0.49	5.02	50.12	0.51	5.13	49.85
S.D.[c]	0.02	0.16	0.74	0.01	0.11	0.53
CV[d]	4.08	3.19	1.48	1.96	2.14	1.06

[a] C_{PA}: PA concentration.
[b] X (μM): mean.
[c] S.D.: standard deviation.
[d] CV: coefficient of variation.

4. Conclusions

In this article we have showed the usefulness of the microfluidic-enzymatic sensor with electrochemical detection, applied to the determination of very low concentrations of pipemidic acid in pharmaceutical samples. This microfluidic biosensor is the first system developed for PA determination in pharmaceutical samples. Our device, coupled to a syringe pumps system, allows operating of fast, selective and sensitive manner. In summary, this sensor provides a cost effective solution to obtain good quantitative information and wide applicability in the pharmaceutical industry as quality control method.

Acknowledgements

The authors wish to thank the Universidad Nacional de San Luis, the Agencia Nacional de Promoción Científica y Tecnológica, and the Consejo Nacional de Investigaciones Científicas y Técnicas (CONICET) for their financial support.

References

[1] J.F. Barrett, J.I. Bernstein, H.M. Krause, J.J. Hilliard, K.A. Ohemeng, Anal. Biochem. 214 (1993) 313–317.
[2] I.D. Meras, A.M. De La Pena, F.S. Lopez, M.I.R. Caceres, Analyst 125 (2000) 1471–1476.
[3] B. Li, Z. Zhang, M. Wu, Mikrochim. Acta 134 (2000) 223–227.
[4] S.-L. Chen, H.-C. Zhao, C.-Y. Sun, N. Lian, L.-P. Jin, Anal. Lett. 35 (2002) 1705–1714.
[5] B. Li, Z. Zhang, L. Zhao, C. Xu, Anal. Chim. Acta 459 (2002) 19–24.
[6] L.M. Du, Y.Q. Yang, Q.M. Wang, Anal. Chim. Acta 516 (2004) 237–243.
[7] A. Egorova, S. Beltyukova, O. Teslyuk, J. Pharm. Biomed. Anal. 21 (1999) 585–590.
[8] C. Liu, H. Zhao, L. Jin, Guangpuxue Yu Guangpu Fenxi 19 (1999) 447–449.
[9] E.J. Llorent-Martínez, P. Ortega-Barrales, A. Molina-Díaz, Anal. Biochem. 347 (2005) 330–332.
[10] F. Cañada-Cañada, A. Espinosa-Mansilla, A. Muñoz de la Peña, J. Sep. Sci. 30 (2007) 1242–1249.
[11] H.-W. Sun, F.-X. Qiao, J. Chromatogr. A 1212 (2008) 1–9.
[12] K.H. Park, H.G. Park, J.H. Kim, K.H. Seong, Biosens. Bioelectron. 22 (2006) 613–620.
[13] V. Srinivasan, V.K. Pamula, R.B. Fair, Anal. Chim. Acta 507 (2004) 145–150.
[14] Z.L. Zhang, C. Crozatier, M. Le Berre, Y. Chen, Microelectron. Eng. 78/79 (2005) 556–562.
[15] D. Psaltis, S.R. Quake, C. Yang, Nature 442 (2006) 381–386.
[16] A.L. deMello, Nature 442 (2006) 394–402.
[17] J. El-Ali, P.K. Sorger, K.F. Jensen, Nature 442 (2006) 403–411.
[18] J. Wang, Z. Chen, P.L.A.M. Corstjens, M.G. Mauk, H.H. Bau, Lab Chip 6 (2006) 46–53.
[19] G.M. Whitesides, Nature 442 (2006) 368–373.
[20] P. Yager, T. Edwards, E. Fu, K. Helton, K. Nelson, M.R. Tam, B.H. Weigl, Nature 442 (2006) 412–418.
[21] K. Sato, M. Tokeshi, T. Odake, H. Kimura, T. Ooi, M. Nakao, T. Kitamori, Anal. Chem. 72 (2000) 1144–1147.
[22] E. Verpoorte, Lab Chip 3 (2003) 42–52.
[23] J.R. Whitaker, C.Y. Lee, Recent advances in chemistry of enzymatic browning: an overview, in: Enzymatic Browning and its Prevention, American Chemical Society, Washington, DC (USA), 1995.
[24] J.R.L. Walker, Enzymatic browning in fruits: its biochemistry and control, in: Enzymatic Browning and its Prevention, American Chemical Society, Washington, DC (USA), 1995.

[25] L. Vámos-Vigyázó, Prevention of enzymatic browning in fruits and vegetables: a review of principles and practice, in: Enzymatic Browning and its Prevention, American Chemical Society, Washington, DC (USA), 1995.
[26] H.S. Mason, Nature 177 (1956) 79–81.
[27] W.H. Vanneste, A. Zuberbüler, Molecular Mechanism of Oxygen Activation, Academic Press, New York, 1974.
[28] K. Lerch, Copper monooxygenases: tyrosinase and dopamine L-hydroxylase, in: Metal Ions in Biological Systems, Marcel Dekker, New York, 1981.
[29] E.I. Solomon, U.M. Sundaram, T.E. Machonkin, Chem. Rev. 96 (1996) 2563–2605.
[30] T. Klabunde, C. Eicken, J.C. Sacchettini, B. Krebs, Nat. Struct. Mol. Biol. 5 (1998) 1084–1090.
[31] L. Bubacco, J. Salgado, A.W.J.W. Tepper, E. Vijgenboom, G.W. Canters, FEBS Lett. 442 (1999) 215–220.
[32] F. Schubert, S. Saini, A.P.F. Turner, F. Scheller, Sens. Actuators B 7 (1992) 408–411.
[33] P. Onnerfjord, J. Emneus, G. Markovarga, L. Gorton, F. Ortega, E. Dominguez, Biosens. Bioelectron. 10 (1995) 607–619.
[34] B. Fuhrmann, U. Spohn, Biosens. Bioelectron. 13 (1998) 895–902.
[35] J. Li, L.S. Chia, N.K. Goh, S.N. Tan, Anal. Chim. Acta 362 (1998) 203–211.
[36] S. Cosnier, J.J. Fombon, P. Labbé, D. Limosin, Sens. Actuators B 59 (1999) 134–139.
[37] M.B. Moressi, M.A. Zón, H. Fernández, G. Rivas, V. Solís, Electrochem. Commun. 1/10 (1999) 472–476.
[38] S. Zhang, H. Zhao, R. John, Anal. Chim. Acta 441 (2001) 95–105.
[39] L. Stancik, L. Macholán, F.W. Scheller, Electroanalysis 7 (1995) 649–651.
[40] K. Streffer, H. Kaatz, C.G. Bauer, A. Makower, T. Schulmeister, F.W. Scheller, M.G. Peter, U. Wollenberger, Anal. Chim. Acta 362 (1998) 81–90.
[41] C.G. Bauer, A.V. Eremenko, E. Ehrentreich-Forster, F.F. Bier, A. Makower, H.B. Halsall, W.R. Heineman, F.W. Scheller, Anal. Chem. 68 (1996) 2453–2458.
[42] S. Ito, S.I. Yamazaki, K. Kano, T. Ikeda, Anal. Chim. Acta 424 (2000) 57–63.
[43] T. Huang, A. Warsinke, T. Kuwana, F.W. Scheller, Anal. Chem. 70 (1998) 991–997.
[44] T. Huang, A. Warsinke, O.V. Koroljova-Skorobogaťko, A. Makower, T. Kuwana, F.W. Scheller, Electroanalysis 11 (1999) 295–300.
[45] F.W. Scheller, F. Schubert, Biosensors: Techniques and Instrumentation in Analytical Chemistry, Elsevier, Amsterdam, 1991.
[46] A.M. Smethurst, W.C. Mann, J. Chromatogr. 274 (1983) 421–427.
[47] K. Fukuhara, Y. Matsuki, J. Chromatogr. 416 (1987) 409–413.
[48] Y.P. Chen, C.Y. Shaw, B.L. Chang, J. Food Drug Anal. 4 (1996) 162–164.
[49] G. Matheis, J.R. Whitaker, J. Food Biochem. 8 (1984) 137–162.
[50] D. Bassil, D.P. Makris, P. Kefalas, Food Res. Int. 38 (2005) 395–402.
[51] P.C. White, N.S. Lawrence, J. Davis, R.G. Compton, Electroanalysis 14 (2002) 89–98.
[52] C.G. Stone, M.F. Cardosi, J. Davis, Anal. Chim. Acta 491 (2003) 203–210.
[53] A.A.J. Torriero, J.J.J. Ruiz Díaz, E. Salinas, E.J. Marchevsky, M.I. Sanz, J. Raba, Talanta 69 (2006) 691–699.
[54] C.J. Cooksey, K. Jimbow, E.J. Land, P.A. Riley, Melanoma Res. 2 (1992) 283–293.
[55] M.J. Picklo, V. Amarnath, D.G. Graham, T.J. Montine, Free Radical Biol. Med. 27 (1999) 271–277.
[56] H.T. Deng, G.J. van Berkel, Electroanalysis 11 (1999) 857–865.
[57] L. Papouchado, G. Petrie, R.N. Adams, J. Electroanal. Chem. 38 (1972) 389–395.
[58] L. Papouchado, G. Petrie, J.H. Sharp, R.N. Adams, J. Am. Chem. Soc. 90 (1968) 5620–5621.
[59] T.E. Young, J.R. Griswold, M.H. Hulbert, I. Melanin, J. Org. Chem. 39 (1974) 1980–1982.
[60] A. Brun, R. Rosset, J. Electroanal. Chem. 49 (1974) 287–300.
[61] D.I. Stom, S.N. Suslov, Biofizika 21 (1979) 40–45.
[62] M.D. Ryan, A. Yueh, C. Wen Yu, J. Electrochem. Soc. 127 (1980) 1489–1495.
[63] M. Friedman, J. Agric Food Chem. 42 (1994) 3–20.
[64] A.A.J. Torriero, E. Salinas, J. Raba, J.J. Silber, Biosens. Bioelectron. 22 (2006) 109–115.
[65] W.J. Albery, Electrode Kinetics, Clarendon Press, Oxford, 1975.